EVALUATING THE NUCLEAR PROPERTIES OF $^{120-130}$Xe ISOTOPES

EVALUACIÓN DE LAS PROPIEDADES NUCLEARES DE LOS ISÓTOPOS DE $^{120-130}$Xe

Yasir Y. Kassim[1], **Rabee B. Alkhayat**[1*] , **Huda H. Kassim**[2], **Fadhil I. Sharrad** [2,3]

[1] University of Mosul, College of Education for Pure Sciences, Departments of Physics, Mosul, Iraq.
[2] University of Kerbala, College of Science, Department of Physics, Karbala, Iraq.
[3] University of Alkafeel, College of Health and Medical Technology, Iraq.

(Recibido: jun./2024. Aceptado: oct./2024)

Abstract

Positive-parity states of $^{120-130}$Xe isotopes were calculated based on the interacting boson model 1 (IBM-1), Semi-Experimental Formula (SEF), and New Empirical Equation (NEE). The calculated results are compared to experimental energy levels, specifically GS, β, and γ bands, in addition to reduced $B(E2)$ transition probabilities. IBM-1, SEF, and NEE accurately represent the comparable energy levels of the GS, γ, and β bands for $^{120-130}$Xe. However, IBM-1 exhibits greater deviations at higher energy levels. The present calculations replicate the experimental results of $^{120-130}$Xe. The potential energy surface (PES) is a nuclear property that determines the ultimate form of nuclei. PES plotting reveals that the $^{120-130}$Xe isotopes are deformed and have a γ–unstable limit.

Keywords: IBM-1, Xe isotopes, SEF, NEE, energy levels.

Resumen

Se calcularon los estados de paridad positiva de los isótopos $^{120-130}$Xe basándose en el modelo de bosón

* khayatrabee@uomosul.edu.iq doi: https://doi.org/10.15446/mo.n70.114834

interactivo 1 (IBM-1), la Fórmula Semiexperimental (SEF) y la Nueva Ecuación Empírica (NEE). Los resultados calculados se comparan con los niveles de energía experimentales, específicamente con las bandas GS, β y γ, además de con las probabilidades de transición reducidas $B(E2)$. El IBM-1, la SEF y la NEE representan con precisión los niveles de energía comparables de las bandas GS, γ y β para el $^{120-130}$Xe. Sin embargo, el IBM-1 muestra mayores desviaciones en los niveles de energía más altos. Los cálculos presentes replican los resultados experimentales de $^{120-130}$Xe. La superficie de energía potencial (PES) es una propiedad nuclear que determina la forma final de los núcleos. El trazado de la PES revela que los isótopos de $^{120-130}$Xe están deformados y tienen un límite γ inestable.

Palabras clave: IBM-1, isótopos de Xe, SEF, NEE, niveles de energía.

1. Introduction

The description of the nuclear structure can be examined with a variety of tools, but the interacting boson model (IBM) is the most crucial. The properties of combined nuclear energy for various nuclei are delineated by the Hamiltonians through the utilization of algebraic group methods. IBM-1 successfully describes the probability of electromagnetic transitions, intermediate nuclei, and the nuclear structure of low-lying states. IBM-1 establishes three dynamically symmetric groups: spherical limit U(5), symmetric rotor SU(3), and γ-unstable O(6), in terms of the unitary group U(6) [1, 2]. Transition zone is a region of the periodic table where Xe isotopes are located; this region is both interesting and complex. Transitionally, the Xe isotopes transform from spherical to deformed nuclei [3]. Various studies have been conducted in recent years on the structure of xenon isotopes. Rawat [4] indicated the symmetry breaking of ^{118,120}Xe by examining the excitation energies of 0_2^+ and 0_3^+ states. Werner et al. [5] performed calculations utilizing the interacting boson model. They revealed that ^{124}Xe

has both O(6) and U(5) symmetry contributions. Saha et al. [6] computed the ground state band of B(E2) and the deduced B(M1) amounts for ^{124}Xe isotope. Systematically, back-bending in the yrast bands was found in the $^{122-130}$Xe isotopes. This unexpected result for ^{124}Xe highlights the subject of whether the O(6) limit is preserved or violated in the adjacent Xe isotopes [7]. The energy levels and B(E2) transitions have been studied for $^{122-142}$Xe isotopes using the IBM-1 and IBM-2 frameworks. These models align well with available experimental data [8]. Li et al. [9] estimated the E2 transition probabilities and EPS plot for $^{128-134}$Xe isotopes. The form of these nuclei varies from spherical to γ-soft. Coquard et al. [10] measured the B(E2) values which indicate that O(5) symmetry is maintained, whereas O(6) symmetry has been violated. Khudher et al. examined several structural properties of $^{120-126}$Xe isotopes using the IBM-1 framework, and their research showed that these nuclei possess gamma-unstable properties [11]. Moreover, the B(E2) transition rates and energy levels of $^{114-134}$Xe isotopes were studied in the U(5)-SO(6) transition region using IBM-1 [12]. The ^{134}Xe nucleus is the best applicant for E(5) symmetry within these nuclei, which have a spherical-γ soft-shape transition. Further, Khudher et al. [13] employed the IBM-1 and IBFM-1 models to examine the positive parity of ^{122}Xe and ^{123}Xe. Gupta and Hamilton [14] studied the energy spectrum and E2 transition of ^{126}Xe isotope using the IBM-1 and Dynamic Pairing Plus Quadrupole (DPPQ) models. Both models are well matched with the experimental results, and the ^{126}Xe has a transition behavior of O(6)-U(5). In neutron-deficient Xe and other nuclei, the change in quadrupole and octupole collectives was examined [15]. Lastly, the IBM-1 model was used to investigate the nuclear structure of the ^{142}Xe isotope. The energy levels and transitions revealed an O(6)–U(5) transition symmetry [16]. The objective of this research is to use the IBM-1 framework to compare the calculated energy levels, transition probabilities B(E2), and potential energy surfaces of a subset of even-even $^{120-130}$Xe isotopes to those obtained from experiments. We also compared SEF and NEE calculations to experimental and IBM-1 results.

2. Basic Calculations

2.1. IBM-1 with Other Computations

The IBM-1 Hamiltonian requires the consideration of nine distinct factors [17, 18].

$$\begin{aligned}\hat{H} = {} & \epsilon_s(s^\dagger \cdot \tilde{s}) + \epsilon_d(d^\dagger \cdot \tilde{d}) \\ & + \sum_{L=0,2,4} \frac{1}{2}(2L+1)^{\frac{1}{2}} C_L \left[[d^\dagger \times d^\dagger]^{(L)} \times [\tilde{d} \times \tilde{d}]^{(L)}\right]^{(0)} \\ & + \frac{1}{\sqrt{2}}\nu_2 \left[[d^\dagger \times d^\dagger]^{(2)} \times [\tilde{d} \times \tilde{s}]^{(2)} + [d^\dagger \times s^\dagger]^{(2)} \times [\tilde{d} \times \tilde{d}]^{(2)}\right]^{(0)} \\ & + \frac{1}{2}\nu_0 \left[[d^\dagger \times d^\dagger]^{(0)} \times [\tilde{s} \times \tilde{s}]^{(0)} + [s^\dagger \times s^\dagger]^{(0)} \times [\tilde{d} \times \tilde{d}]^{(0)}\right]^{(0)} \\ & + \frac{1}{2}u_0 \left[[s^\dagger \times s^\dagger]^{(0)} \times [\tilde{s} \times \tilde{s}]^{(0)}\right]^{(0)} \\ & + u_2 \left[[d^\dagger \times s^\dagger]^{(2)} \times [\tilde{d} \times \tilde{s}]^{(2)}\right]^{(0)}.\end{aligned} \tag{1}$$

It is important to acknowledge that the aforementioned equation can also be expressed in multipolar form:

$$\hat{H} = \epsilon\hat{n}_d + a_0\hat{P}\cdot\hat{P} + a_1\hat{L}\cdot\hat{L} + a_2\hat{Q}\cdot\hat{Q} + a_3\hat{T}_3\cdot\hat{T}_3 + a_4\hat{T}_4\cdot\hat{T}_4. \tag{2}$$

The operators are defined as:

$$\left.\begin{aligned}\hat{n}_d &= (d^\dagger \cdot \tilde{d}) \\ \hat{p} &= \frac{1}{2}\left[\left(\tilde{d}\cdot\tilde{d}\right) - (\tilde{s}\cdot\tilde{s})\right] \\ \hat{L} &= \sqrt{10}\,[d^\dagger \times \tilde{d}]^1 \\ \hat{Q} &= \left[d^\dagger \times \tilde{s} + s^\dagger \times \tilde{d}\right]^{(2)} + \chi\left[d^\dagger \times \tilde{d}\right]^{(2)} \\ \hat{T}_r &= \left[d^\dagger \times \tilde{d}\right]^{(r)}\end{aligned}\right]. \tag{3}$$

Where $\hat{n}_d$ is the d-boson operator, $\hat{p}$ is the operator for pairing, $\hat{L}$ is the operator for angular momentum, $\hat{Q}$ is the operator for quadrupole, and $\hat{T}_r$ is the operator for octupole and hexadecapole.

The U(6) group determines the symmetry of the IBM-1. This group consists of three subgroups: U(5) for vibration, SU(3) for rotation, and O(6) for soft nuclei [19], which are given as:

$$U(6) \supset \left\{ \begin{array}{c} U(5) \supset O(5) \\ SU(3) \\ O(6) \supset O(5) \end{array} \right\} \supset O(2). \tag{4}$$

Therefore, the eigenvalues of the U(6) subgroups are given by

$$\left.\begin{array}{ll} E(n_d,\nu,L) = \varepsilon n_d + \frac{a_1}{12} n_d(n_d+4) + \left(\frac{a_3}{7} - \frac{a_1}{10} - \frac{3a_4}{70}\right)\nu(\nu+3) + \frac{1}{14}(a_4-a_3)L(L+1) & \mathrm{U(5)} \\ E(\lambda,\mu,L) = \frac{a_2}{2}\left(\lambda^2+\mu^2+\lambda\mu+3(\lambda+\mu)\right) + \left(a_1 - \frac{2a_2}{8}\right)L(L+1) & \mathrm{SU(3)} \\ E(\sigma,\tau,L) = \frac{a_0}{4}(N-\sigma)(N+\sigma+4) + \frac{a_3}{2}\tau(\tau+3) + \left(a_1 - \frac{a_3}{10}\right)L(L+1) & \mathrm{O(6)} \end{array}\right], \tag{5}$$

ε, a_0, and a_2 are parameters representing energy, pairings, and quadrupoles, respectively. Multiple nuclei have the ability to move between two or more of the previously mentioned boundaries. The energy ratio $R = \frac{E(4_1^+)}{E(2_1^+)}$ can be used to predict the behavior of even-even nuclei, where $E(4_1^+)$ and $E(2_1^+)$ are the second and first excitation levels of energy, respectively.

Several equations, including the Semi-Experimental Formula (SEF) [20] and the New Empirical Equation (NEE) [21], were recently derived due to the difficulty of investigating the nuclear structure, particularly deformed nuclei. The formula for the SEF used in determining the GSB is given by:

$$E(I) = A_1\left[e^{A_2 I} - A_3\right], \tag{6}$$

The measured energies of GSB predicted A_1, A_2, and A_3. The bands of γ and β are computed as:

$$E(I) = E_0 + (A_1 + B)\left[e^{A_2 I} - A_3\right], \tag{7}$$

The E_0 and B are calculated from γ and β-bands. Correspondingly, the NEE formula was employed to compute all necessary calculation parameters. Regarding the GSB band

$$E(I) = \frac{A_1 I(I+1)}{A_2(I+1) + I A_3}, \tag{8}$$

the γ and β bands are calculated as

$$E(I) = E_0 + \frac{(A_1 + B)I(I+1)}{A_2(I+1) + IA_3}. \tag{9}$$

2.2. The Probability of Quadrupole Transition B(E2)

The nuclear structure can be comprehended by utilizing the electric quadrupole transition. The $T^{(E2)}$ operator can be utilized to calculate the $B(E2)$ strength [19, 22]:

$$B\left((E2)_{I_i \to I_f}\right) = \frac{1}{2L_i + 1} \left|\langle I_f \| T^{(E2)} \| I_i \rangle\right|^2, \tag{10}$$

where

$$T^{(E2)} = \alpha_2 \left[d^\dagger \times s + s^\dagger \times d\right] + \beta_2 \left[d^\dagger \cdot d\right] = e_B \hat{Q}. \tag{11}$$

Where e_B signifies the boson's effective charge, the $(s^\dagger, d^\dagger)$ represents the creation operator, and (s, d) represents the annihilation operator. Here, $\alpha_2 = e_B$ and $\beta_2 = \chi\alpha_2$. The electric quadrupole transitions formula is given by

$$B(E2) = \frac{0.5657}{T_{1/2}^{\cdot\cdot}(ps) \times E_\gamma^5 \text{ (MeV)}} e^2 b^2, \tag{12}$$

E_γ is the gamma energy and $T_{1/2}^{\cdot\cdot}$ is a half-time.

2.3. Potential energy surface (PES)

The IBM-1 is originally described using the terminology of creation and annihilation boson operators. The state of intrinsic coherence ($|N, \beta, \gamma\rangle$) is expressed as a state of bosons. To produce the coherent state, the creation operators ($b_c^\dagger$) operate on a state of boson vacuum $|0\rangle$ as follows [23]

$$\mid N, \beta, \gamma\rangle = \frac{1}{\sqrt{N!}} (b_c^\dagger)^N |0\rangle, \tag{13}$$

$$b_c^\dagger = \frac{1}{\sqrt{1+\beta^2}} \left\{ s^\dagger + \beta \left[\cos\gamma (d_0^\dagger) + (0.5)^{\frac{1}{2}} \sin\gamma (d_2^\dagger + d_{-2}^\dagger) \right] \right\}. \tag{14}$$

The PES is defined in terms of β and γ for the purpose of estimating the expected value of the Hamiltonian for the intrinsic boson state [16] as follows:

$$E(N,\beta,\gamma) = \frac{N\varepsilon_d\beta^2}{(1+\beta^2)} + \frac{N(N+1)}{(1+\beta^2)^2}[\alpha_1\beta^4 + \alpha_2\beta^3\cos 3\gamma + \alpha_3\beta^2 + \alpha_4], \quad (15)$$

the α's are associated with the coefficients C_L, ν_2, ν_0, u_2, and u_0 of Eq. 1

3. Results and Discussion

The subsequent section provides a discussion on the GS, γ, and β bands computed by the IBM-1, SEF, and NEE frameworks for the $^{120-130}$Xe isotopes.

For a basic stage in the calculation process, the ratio $R_{4/2}$ for each isotope is deduced. Based on the preliminary results in Table 1, the $^{120-130}$Xe isotopes have dynamical states that range from U(5) to O(6). The $R_{4/2}$ values of Xe isotopes, lowest energy levels change as a consequence of mass number. In addition, Table 2 displays the IBM-1, a_0, a_1, and a_3 coefficient values for $^{120-130}$Xe isotopes. The parameters a_0, a_1, and a_3 correspond, respectively, to the pairing strength, angular momentum, and octupole interaction among bosons. Tables 3, 4, and 5 exhibit, respectively, the computed GS, β, and γ band values for the SEF and NEE equations for the investigated isotopes.

Isotopes	^{120}Xe	^{122}Xe	^{124}Xe	^{126}Xe	^{128}Xe	^{130}Xe
$R_{4/2}$	2.468	2.501	2.483	2.424	2.333	2.247

TABLE 1. *The values of $R_{4/2}$ for $^{120-130}$Xe*

Root-mean-square deviation (RMSD) [24] was applied to estimate the difference amongst IBM-1, SEF, and NEE energy levels and experimental data. Table 6 displays the RMSD results for the three bands. The experimental results [25–30] for the GS, β, and γ bands appeared comparable to the IBM-1, SEF, and NEE computations shown in Figures 1–3 respectively.

The experimental, IBM-1, SEF, and NEE results for GSB are shown in Figure 1. It is apparent that the IBM-1, SEF, and

Isotopes	N	a_0	a_1	a_3
^{120}Xe	10	0.0826	0.0121	0.1785
^{122}Xe	9	0.1150	0.0158	0.1690
^{124}Xe	8	0.1410	0.0193	0.1700
^{126}Xe	7	0.1642	0.0225	0.1810
^{128}Xe	6	0.2260	0.0252	0.2078
^{130}Xe	5	0.2960	0.0308	0.2504

TABLE 2. *IBM-1 data for Xe isotopes*

	SEF			NEE		
Isotopes	A_1	A_2	A_3	A_1	A_2	A_3
^{120}Xe	8.6544	0.0306	1.0307	0.0889	0.6879	–0.1226
^{122}Xe	2.6455	0.0790	1.0505	0.0780	0.3273	0.0698
^{124}Xe	7.8621	0.0344	1.0271	0.0821	0.7410	–0.2228
^{126}Xe	9.6705	0.0296	1.0188	0.1118	0.7120	–0.1101
^{128}Xe	6.3972	0.0395	1.0022	0.0806	0.7869	–0.2937
^{130}Xe	7.8760	0.0324	0.9850	0.1370	0.8130	–0.1572

TABLE 3. *GSB results of SEF and NEE for Xe isotopes*

	b-band			γ-band	
Isotopes	N	E_0	B	E_0	B
^{120}Xe	10	1.0903	–2.4757	0.5859	0.1520
^{122}Xe	9	1.3760	–0.6401	0.8009	0.3766
^{124}Xe	8	1.4520	–2.9325	0.6349	0.2508
^{126}Xe	7	1.6456	–3.9865	0.4266	0.9247
^{128}Xe	6	1.8549	–6.3972	0.5031	0.3278
^{130}Xe	5	1.8956	–0.4995	0.5945	2.7697

TABLE 4. *SEF variables are in MeV for β and γ bands*

NEE computations match the current experimental observations. In comparison to the IBM-1 and SEF computations, the SEF formula provides a more accurate depiction of the ground-state energy level calculations. The ^{128}Xe isotope IBM-1 computations found a maximum RMSD inaccuracy. In NEE calculations, the greatest

	b-band			γ-band	
Isotopes	N	E0	B	E0	B
120	10	0.9161	0.0827	0.3350	0.1500
122	9	1.2829	0.0826	0.4314	0.0573
124	8	1.3325	0.0481	0.0727	0.2102
126	7	1.2670	–0.0129	0.3253	0.1618
128	6	2.0814	–0.1746	0.5325	0.1771
130	5	1.7275	–0.6741	0.1329	–0.4915

TABLE 5. *NEE variables are in MeV for β and γ bands*

Xe Isotopes	GSB			γ-band			β-band		
	IBM-1	SEF	NEE	IBM-1	SEF	NEE	IBM-1	SEF	NEE
^{120}Xe	0.0352	0.0552	0.0833	0.4150	0.0713	0.0883	0.2275	0.0117	0.0083
^{122}Xe	0.1057	0.0147	0.0035	0.3098	0.1232	0.0514	—	—	—
^{124}Xe	0.2177	0.0806	0.1319	0.5019	0.0767	0.1324	0.1971	0.0259	0.0372
^{126}Xe	0.3749	0.0898	0.1186	0.6439	0.0607	0.0686	0.2170	0.0759	0.0724
^{128}Xe	0.6706	0.0919	0.1228	0.5466	0.2833	0.2746	0.0829	0.2221	0.3198
^{130}Xe	0.1510	0.1531	0.1555	0.7584	0.0773	0.0722	0.2122	0.0641	0.1142

TABLE 6. *RMSD values for GS, γ, and β bands*

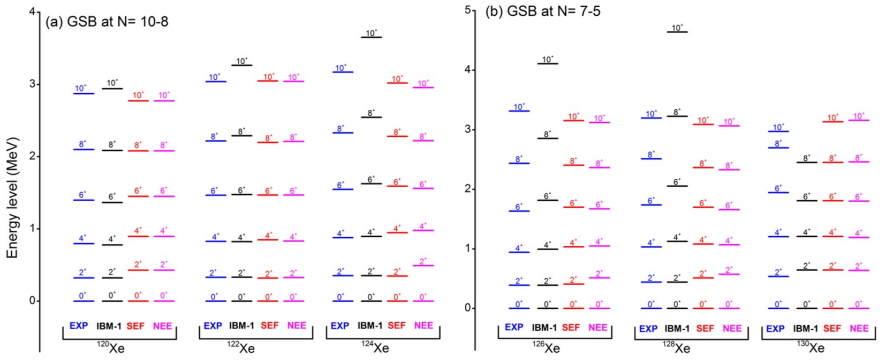

FIGURE 1. *GSB values for the $^{120-130}$Xe isotopes [25–30]*

RMSD for ^{130}Xe isotopes is roughly 0.1555. SEF analyses show the minimal errors, though. Unlike the assumptions of IBM-1 and NEE, the RMSD errors of SEF calculations remain relatively unchanged as the level of excited states keeps increasing.

As shown in Figure 2, the RMSD errors of the IBM-1 model for Xe isotopes are greater than those of the SEF and NEE estimates for the β-bands. For SEF and NEE calculations, the energy gap between states in the ^{120}Xe to ^{130}Xe isotopes is equivalent, but for IBM-1 results, it is higher. The RMSD error of ^{120}Xe NEE estimations is also smaller than those of SEF and IBM-1. In general, the SEF, NEE, and IBM-1 calculations closely replicated the experimental β-band energy levels accurately; however, for higher states, significant discrepancies were observed, particularly in the IBM-1 calculations. SEF and NEE estimates could not be determined for ^{122}Xe because experimental data were insufficient.

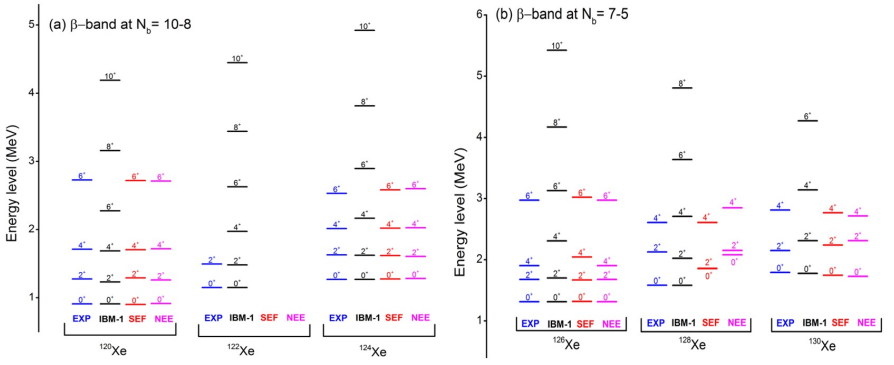

FIGURE 2. *β-band values for the $^{120-130}Xe$ isotopes [25–30]*

Figure 3 displays the estimated and observed values [25–30] of the γ-bands for the ^{120}Xe to ^{130}Xe isotopes. The highest error for the ^{130}Xe isotope based on IBM-1 computations is around 0.7584. In spite of this, the SEF and NEE estimations match the published data. However, in the case of ^{120}Xe, the NEE and SEF calculations were in close agreement with the experimental values in comparison to the IBM-1 computation. The NEE calculation yields a smaller error for ^{122}Xe than the SEF and IBM-1 estimates. The SEF calculations for the ^{124}Xe isotope are much closer to the experimental values than the IBM-1 and NEE calculations. The ratio of the IBM-1 calculation to the experimental values are smaller than that of the SEF and NEE calculations, and the RMSD error

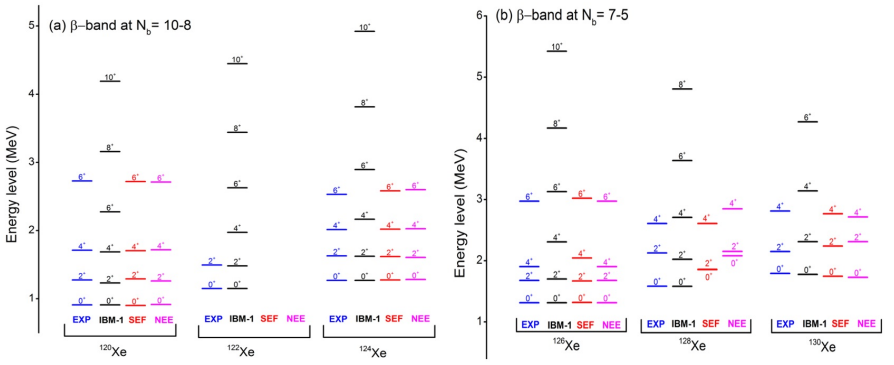

FIGURE 3. *γ-band values for the $^{120-130}$Xe isotopes [25–30]*

for the ^{126}Xe and ^{130}Xe isotopes is approximately the same. We noticed that the IBM-1 calculation for the spacing rates of ^{126}Xe, ^{128}Xe, and ^{130}Xe isotopes was less aligned with the literature data than the SEF and NEE calculations.

Furthermore, in the IBM-1 calculations, the representations of the energies of the 3^+, 4^+, 5^+, and 6^+ states are not accurately represented in the IBM-1, particularly in γ-bands, because the nuclei have O(6)-U(5) transitional dynamical symmetry. In the O(6) region, the 3^+ and 4^+ states have the same value and are less than the 6^+ state, while in U(5), the energy states 3^+ and 4^+ are equal to the energy state 6^+. The neutrons and protons are not distinguished in the IBM-1 model, and each nucleon interacts with others, making the nuclear structure more complex. For this reason, the IBM-1 fails at high energy levels.

We observed that the IBM-1 calculations are more accurate than other calculations in the low-lying states. In the β-band energy levels, the NEE calculations are more accurate than IBM-1 and SEF calculations, except for ^{128,130}Xe isotopes. For γ-band energy levels, the SEF calculations are more accurate than IBM-1 and NEE results. In addition, the IBM-1 calculations fail in the highly excited state. The above discussion is for $I \leq 10$, and further research is required to confirm which of these estimates more closely matches the experimental data that is currently available for $I \geq 20$.

The e_B values required to reproduce the experimental $B(E2;_{2_1^+ \to 0_1^+})$ are provided in Table 7.

Isotopes	N	e_B (e^2b^2)
^{120}Xe	10	0.1111
^{122}Xe	9	0.1094
^{124}Xe	8	0.1030
^{126}Xe	7	0.1009
^{128}Xe	6	0.1238
^{130}Xe	5	0.1280

TABLE 7. *Effective charge values for nuclei $^{120-130}Xe$*

Table 7 shows that the e_B values decrease with increasing mass number in $^{120-126}$Xe isotopes, and for ^{128,130}Xe isotopes, show that the e_B values increase with increased mass number. In addition, comparisons of experimental and calculated $B(E2)$ results are presented in Tables 8, 9, and 10 for all nuclei under consideration.

$J_i \to J_f$	^{120}Xe		^{122}Xe	
	IBM-1	EXP.	IBM-1	EXP.
$2_1^+ \to 0_1^+$	0.3460	0.346	0.2800	0.280
$2_2^+ \to 0_1^+$	0.0483	—	0.0392	—
$4_1^+ \to 2_1^+$	0.4766	0.440	0.3829	0.3870
$4_2^+ \to 2_1^+$	0.0385	—	0.0307	—
$6_1^+ \to 4_1^+$	0.5272	0.4780	0.4188	0.3960
$6_1^+ \to 4_2^+$	0.0245	—	0.0211	—
$8_1^+ \to 6_1^+$	0.5347	0.4000	0.4177	0.4670
$8_1^+ \to 6_2^+$	0.0289	—	0.0255	—
$10_1^+ \to 8_1^+$	0.5133	0.3770	0.3912	0.4320
$6_2^+ \to 6_1^+$	0.1701	—	0.1329	—
$3_1^+ \to 4_1^+$	0.1507	—	0.1197	—
$3_1^+ \to 2_1^+$	0.0525	—	0.0419	—

TABLE 8. *Theoretical and experimental B(E2) values in e^2b^2 units for the $^{120-122}Xe$ isotopes [25, 26]*

Tables 8, 9, and 10 demonstrate that, with the exception of a few instances, the majority of results obtained in IBM-1

are coherent with the obtainable experimental data, and the $B(E2)$ transition values increase with decreasing boson number to $B(E2;_{8_1^+\to 6_1^+})$ and decrease at $B(E2;_{10_1^+\to 8_1^+})$ in ^{120,126}Xe isotopes while decreasing at $B(E2;_{8_1^+\to 6_1^+})$ in ^{128,30}Xe isotopes. The contour lines in the plane resulting from (N, β, γ) for ^{120,130}Xe are shown in Figure 4. For the majority of Xe nuclei considered, the energy surfaces have a triaxial shape and are between $0 < \gamma < 60$. In summary, the Xe nuclei exhibit no rapid structural change and retain their γ-softness.

$J_i \to J_f$	^{124}Xe		^{126}Xe	
	IBM-1	EXP.	IBM-1	EXP.
$2_1^+ \to 0_1^+$	0.1920	0.1920	0.1540	0.1590
$2_2^+ \to 0_1^+$	0.0027	0.0026	0.00217	0.0020
$4_1^+ \to 2_1^+$	0.2600	0.2491	0.2057	0.2640
$4_2^+ \to 2_1^+$	0.0206	0.0003	0.0160	0.0018
$4_2^+ \to 2_2^+$	0.1467	0.1620	0.1135	0.1339
$6_1^+ \to 4_1^+$	0.2800	0.2940	0.2167	0.2740
$8_1^+ \to 6_1^+$	0.2727	0.2437	0.2036	—
$10_1^+ \to 8_1^+$	0.2462	0.0773	0.1731	—
$2_2^+ \to 2_1^+$	0.2600	0.1420	0.2057	0.1621
$2_3^+ \to 2_1^+$	0.0031	0.0024	0.0026	0.0004
$4_2^+ \to 4_1^+$	0.1333	0.1254	0.1032	0.1062
$3_1^+ \to 4_1^+$	0.0799	0.0964	0.0618	0.0829
$3_1^+ \to 2_1^+$	0.0281	0.0035	0.0218	0.0036
$3_1^+ \to 2_2^+$	0.2000	0.3454	0.1548	0.2091

TABLE 9. *Theoretical and experimental B(E2) values in e^2b^2 units for the $^{124-126}$Xe isotopes [27, 28]*

$J_i \to J_f$	^{124}Xe		^{126}Xe	
	IBM-1	EXP.	IBM-1	EXP.
$2_1^+ \to 0_1^+$	0.1839	0.1840	0.1475	0.1481
$2_2^+ \to 0_1^+$	0.0258	0.0031	0.0205	—
$2_2^+ \to 2_1^+$	0.2408	—	0.1872	0.0002
$4_1^+ \to 2_1^+$	0.2408	0.2376	0.1872	0.0002
$4_2^+ \to 2_1^+$	0.0180	—	0.0131	—
$4_2^+ \to 2_2^+$	0.1285	0.1069	0.0944	0.0001
$6_1^+ \to 4_1^+$	0.2452	0.2339	0.1802	—
$6_1^+ \to 4_2^+$	0.0194	—	0.0190	0.0001
$8_1^+ \to 6_1^+$	0.2174	0.3220	0.1430	—
$8_1^+ \to 6_2^+$	0.0256	—	0.0262	—
$10_1^+ \to 8_1^+$	0.1651	0.0009	—	—
$6_2^+ \to 6_1^+$	0.0692	—	0.1245	—
$3_1^+ \to 4_1^+$	0.0484	0.2376	0.0355	—
$3_1^+ \to 2_1^+$	0.0246	0.0146	0.0179	—

TABLE 10. *Theoretical and experimental B(E2) values in e^2b^2 units for the $^{128-130}Xe$ isotopes [29, 30]*

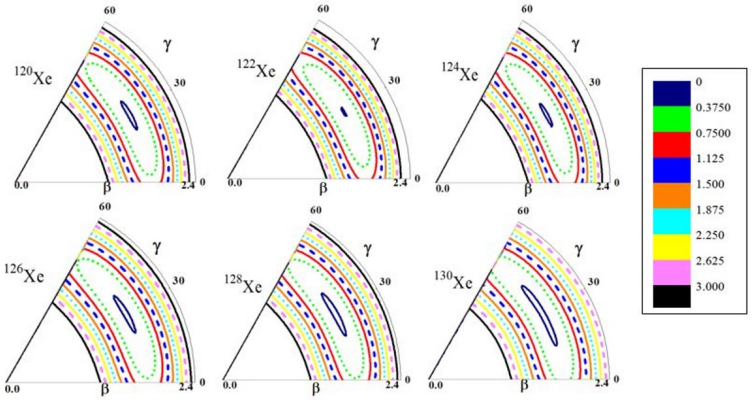

FIGURE 4. *Surface maps of potential energy for the $^{120-130}$Xe isotopes*

4. Conclusion

The IBM-1, SEF, and NEE methods were used to determine the ground state and other state energies. Based on the preliminary results, $^{120-130}$Xe isotopes exhibit dynamical states that range from U(5) to O(6). The $R_{4/2}$ values of Xe isotopes' lowest energy levels change as a consequence of mass number. The SEF method presents a better representation of the ground state band in comparison to the IBM-1 and NEE methods. SEF analyses show the minimal errors. Unlike the assumptions of IBM-1, the RMSD errors of SEF and NEE calculations remain relatively unchanged as the level of excited states keeps increasing. The SEF and NEE calculations for the β-bands are smaller than the RMSE errors of the IBM-1 model for Xe isotopes. The energy gap between states in the $^{120-130}$Xe isotopes is approximately the same for SEF and NEE calculations, whereas it is greater for IBM-1 results. The results of the experiment closely match the NEE calculation for ^{120}Xe compared to the SEF and IBM-1 calculations. Overall, the calculations of SEF, NEE, and IBM-1 closely resembled the experimental γ-band energy levels; however, there were significant variations for higher states, especially in the IBM-1 calculations. There were not enough experimental data available to determine SEF and NEE for the ^{122}Xe isotope in the β-band. The representations of the energies of the 3^+, 4^+, 5^+, and 6^+ states are not accurately represented in the IBM-1, particularly in γ-bands, because the nuclei have O(6)-U(5) transitional dynamical symmetry, especially ^{128,130}Xe isotopes. While in U(5) the energy levels 3^+ and 4^+ are equal to the energy state of 6^+. These states have the same value and are less than 6^+ in O(6). The IBM-1 results for reduced transition probabilities $B(E2)$ are consistent with the existing experimental data. For ^{128,130}Xe isotopes, the e_B values increase as the mass number increases, while for the other isotopes, the e_B values decrease. The $B(E2)$ values increase at $B(E2;_{8_1^+\rightarrow 6_1^+})$ and then decrease at $B(E2;_{10_1^+\rightarrow 8_1^+})$ as the boson number decreases. The potential energy surface (PES) is a nuclear property that determines the ultimate form of nuclei. PES plotting reveals that the $^{120-130}$Xe isotopes are deformed, have a triaxial shape, and are

between $0 < \gamma < 60$. In summary, the Xe nuclei exhibit no rapid structural changes and retain their γ-softness.

References

[1] P. Cejnar, J. Jolie, and et al., Rev. Mod. Phys. **82**, 2155 (2010).

[2] R. Kumar, S. Sharma, and J. Gupta, Armenian J. Phys. **3**, 150 (2010).

[3] R. Casten and E. McCutchan, J. Phys G: Nucl. Part. Phys. **34**, R285 (2007).

[4] B. Rawat and P. Chattopadhyay, Pramana - J. Phys. **53**, 911 (1999).

[5] V. Werner, H. Meise, and et al., Nuclear Physics A **692**, 451 (2001).

[6] B. Saha, A. Dewald, and et al., Phys. Rev. C **70**, 034313 (2004).

[7] G. Rainovski, N. Pietralla, and et al., Phys. Lett. B **683**, 11 (2010).

[8] N. Turkan and I. Maras, Math. Comput. Appl. **16**, 467 (2011).

[9] Z. P. Li, T. Nikšić, and et al., Phys. Rev. C **81**, 034316 (2010).

[10] L. Coquard, G. Rainovski, and et al., Phys. Rev. C **83**, 044318 (2011).

[11] H. Khudher, A. Hasan, and F. Sharrad, Ukr. J. Phys. **62**, 152 (2018).

[12] M. Jafarizadeh, N. Fouladi, and et al., Braz. J. Phys. **43**, 34 (2013).

[13] H. H. Khudher, A. K. Hasan, and F. I. Sharrad, Chinese J. Phys. **55**, 1754 (2017).

[14] J. B. Gupta and J. H. Hamilton, Phys. Rev. C **104**, 054325 (2021).

[15] K. Nomura, R. Rodríguez-Guzmán, and L. M. Robledo, Phys. Rev. C **104**, 054320 (2021).

[16] A. A. Sabry, Kuwait J. Sci. **50**, 204 (2023).

[17] H. El-Gendy, Nucl. Phys. A **1006**, 122117 (2021).

[18] A. Mohammed-Ali, R. Alkhayat, and et al., Rev. Mex. Fís. **68**, 060401 (2022).

[19] A. Al-Nuaimi, R. Alkhayat, and et al., Karbala Int. J. Mod. Sci. **8**, 391 (2022).

[20] M. A. Al-Jubbori, H. H. Kassim, and et al., Nucl. Phys. A **955**, 101 (2016).

[21] M. A. Al-Jubbori, F. S. Radhi, and et al., Nucl. Phys. A **971**, 35 (2018).

[22] H. Kassim, A. Elbndag, and et al., Momento **69**, 101 (2024).

[23] F. Ali, M. Al-Jubbori, and et al., Momento **68**, 86 (2024).

[24] F. X. Xu, C. S. Wu, and J. Y. Zeng, Phys. Rev. C **40**, 2337 (1989).

[25] K. Kitao, Y. Tendow, and A. Hashizume, Nucl. Data Sheets **96**, 241 (2002).

[26] T. Tamura, Nucl. Data Sheets **108**, 455 (2007).

[27] J. Katakura and Z. Wu, Nucl. Data Sheets **109**, 1655 (2008).

[28] H. Iimura, J. Katakura, and S. Ohya, Nucl. Data Sheets **180**, 1 (2022).

[29] Z. Elekes and J. Timar, Nucl. Data Sheets **129**, 191 (2015).

[30] B. Singh, Nucl. Data Sheets **96**, 1 (2002).